Hofmeister Effects on Electron-Transfer Reactions of 1-Pyrenesulfonic Acid Radical Cation with Nucleophilic Anions in Nafion Membranes

Takashi Tachikawa, Ramasamy Ramaraj,† Mamoru Fujitsuka, and Tetsuro Majima*

The Institute of Scientific and Industrial Research (SANKEN), Osaka University, Mihogaoka 8-1, Ibaraki, Osaka 567-0047, Japan

Received: September 28, 2004; In Final Form: November 28, 2004

The electron-transfer reaction from nucleophilic anions such as SCN^-, N_3^-, I^-, and Br^- to the 1-pyrenesulfonic acid radical cation ($Py^{\bullet+}SA^-$) generated via a resonant two-photon ionization process in the Nafion membranes was investigated with transient absorption measurements. The apparent quenching rates observed in the Nafion membrane (k_q^{Nf}) were almost 2−4 orders smaller than those observed in the bulk solutions (k_q^{bulk}). The attenuation factor (AF), which is defined as $\log(k_q^{Nf}/k_q^{bulk})$, decreased in the order $SCN^- > N_3^- > I^- > Br^-$. This interesting behavior was interpreted in terms of the anionic Hofmeister effects. The effects of hydrophobic organic cations such as tetrabutylammonium ion (Bu_4N^+) and tetraethylammonium ion (Et_4N^+) exchanged into the Nafion membranes were also examined.

Introduction

Nafion membranes have been widely used in biological and technological areas because of their cation exchange and ion-conducting properties, and high thermal and chemical stability.[1−4] In addition to being commonly used in fuel cells, they have been used as separators in the electrolytic recovery of chromium from waste plating solutions. In diffusion cells, the electroneutrality of solutions needs to be maintained either by diffusion of protons in the opposite direction of the cations or by diffusion of anions in the same direction as the cations. As is well-known, at low ionic strength and neutral pHs, anion transport through a Nafion membrane is suppressed due to the electrostatic-repulsion forces between the anions and the sulfonate ($-SO_3^-$) fixed-charge sites in the membrane.[5−8] However, if the electrostatic repulsion in the membrane is suppressed, anions can readily diffuse through a Nafion membrane. The anions may diffuse together with cations through the membrane as ion pairs. In addition, amphiphilic media such as micelles and perfluorosulfonated ionomer membranes have been used as models for understanding the photochemistry in vesicles and biological membranes.[1,9]

To date, pyrene (Py) and its numerous derivatives have been widely used to probe the microscopic environment and the dynamic behavior in the Nafion membrane.[10−15] Their excellent probing abilities are largely due to the photophysical and photochemical properties involving fluorescence and formation of excimer complexes. Kuczynski and co-workers found that $I_3/I_1 = 0.8$, where I_1 and I_3 are the fluorescence intensities of the first and third vibronic bands, respectively, for Py in the Nafion-H^+ membrane from methanolic solutions, is a value situated between that expected for the highly nonpolar fluorocarbon environment of the matrix and that of the polar clusters.[10] Lee and Meisel investigated Nafion-H^+ incorporated with Py from water as well as from *tert*-butyl alcohol solutions.[11] They determined the I_3/I_1 values of 0.70 and 0.94 in Nafion/water and Nafion/*tert*-butyl alcohol, respectively. Py is considered to be located in sulfonic acid clusters, but close to the interface with the perfluorocarbon matrix rather than near the cluster center. Also, Py excimer formation occurred in an alcohol-swollen but not in a water-swollen Nafion membrane. More recently, Robertson and Yeager studied the time dependence of Py incorporation in both sulfonate and carboxylate Nafion forms.[14] They determined the I_3/I_1 values (0.75−0.79 for sulfonate forms) and also concluded that Py preferentially resides in the interfacial regions.

Although numerous experiments have been conducted to clarify the microenvironment of the Nafion membrane and the bimolecular reaction in the Nafion membrane, there is no report on the bimolecular reaction dynamics of anions such as halide ions in the Nafion membrane. The reason is simply due to the fact that the lifetime of Py in the singlet excited state, which ranges from a few tens to a few hundreds of nanoseconds, is too short to detect the bimolecular reaction with anions due to their low concentration and mobility in the Nafion membrane. On the other hand, the Py radical cation ($Py^{\bullet+}$) and the dimer radical cation ($Py_2^{\bullet+}$) can provide information on the dynamics in the time range of 0.1−100 μs. Recently, our research group clarified the formation and decay of the 1-pyrenesulfonic acid radical cation ($Py^{\bullet+}SA^-$) and $PySA^-$ dimer radical cation ($(PySA^-)_2^{\bullet+}$) included in β- and γ-cyclodextrins during the 355-nm resonant two-photon ionization of $PySA^-$ with the transient absorption measurements.[16] Kiwi et al. studied the formation of the anthracene radical cation in H^+-, Na^+-, Fe^{2+}-, and Fe^{3+}-Nafion membranes via a two-photon ionization process with the transient absorption measurement. They directly observed the electron transfer from Fe^{2+} to the anthracene radical cation in the Nafion membrane.[17]

In the present study, we have investigated the electron-transfer reaction from nucleophilic anions such as SCN^-, N_3^-, I^-, and Br^- to $Py^{\bullet+}SA^-$, which is generated via a resonant two-photon ionization process, in Nafion membranes with transient absorption measurements. The significant difference between the quenching rates of $Py^{\bullet+}SA^-$ by anions in the Nafion membranes

* Address correspondence to this author. Phone: +81-6-6879-8495. Fax: +81-6-6879-8499. E-mail: majima@sanken.osaka-u.ac.jp.

† Guest Professor in 2004 from the School of Chemistry, Madurai Kamaraj University, Madurai 625 021, India.

10.1021/jp045606e CCC: $30.25
Published on Web 01/21/2005

and in the bulk water was interpreted in terms of the anionic Hofmeister effects. The effects of hydrophobic organic cations such as tetrabutylammonium ion (Bu_4N^+) and tetraethylammonium ion (Et_4N^+) exchanged into the Nafion membranes were also examined.

Experimental Section

Chemicals. The Nafion membrane (Nafion-117) with an equivalent weight of 1100 g equiv^{-1} and a thickness of 0.007 in. (178 μm) was obtained from Aldrich. Sodium 1-pyrenesulfonic acid (NaPySA) (Molecular Probes) was used without further purification. NaSCN (Nakarai Tesque, 99%), NaN_3 (Nakarai Tesque, 98%), NaI (Nakarai Tesque, 99.5%), NaBr (Nakarai Tesque, 99.5%), and $FeSO_4 \cdot 7H_2O$ (Nakarai Tesque, 99%) salts were used without further purification as the source of ions. Sodium hydroxide (NaOH) (Wako, 96%), tetraethylammonium bromide (Et_4NBr) (Wako, 98%), and tetrabutylammonium bromide (Bu_4NBr) (Aldrich, 99%) were used without further purification as the source of cations exchanged into the Nafion membranes. Milli-Q water was used as solvent.

Preparation of $PySA^-$-Loaded Nafion Membranes. The Nafion membranes (6 mm $\times$ 20 mm) were immersed in concentrated nitric acid while stirring at 60 °C for 24 h. The acid was then decanted, and the membranes were placed sequentially in aqueous solutions of 60%, 40%, and 20% nitric acid, each for 1 h with stirring, followed by washing thoroughly with clean water until neutral.[18]

For substitution of cations, the Nafion-H^+ membranes (6 mm $\times$ 20 mm) were immersed in aqueous solutions of NaOH (1 M), Et_4NBr (0.1 M), and Bu_4NBr (0.1 M) at room temperature for 48 h.[19]

Purified H^+- and cation-substituted Nafion membranes were soaked in methanolic solutions of $PySA^-$ (1×10^{-2} M) for 24 h at room temperature. The membranes were then washed with methanol several times to clean the membrane surface. The adsorption of $PySA^-$ in the membranes was examined by UV/visible absorption spectral measurements. The $PySA^-$-loaded Nafion membranes were immersed in the appropriate solutions (1×10^{-3} dm^{-3}) for 15 min before laser excitation.

Steady-State UV/Visible Absorption and Fluorescence Measurements. The steady-state UV/visible absorption and fluorescence spectra were recorded on a Shimadzu UV-3100 spectrophotometer and a Hitachi 850 spectrofluorometer, respectively.

Transient Absorption Measurements. Transient absorption measurements were performed by using the third harmonic generation (355 nm, 5 ns fwhm) from a Q-switched Nd:YAG laser (Continuum, Surelite II-10) for the excitation operated with temporal control by a delay generator (Stanford Research Systems, DG535). The irradiation energy was directly measured with a power meter. The analyzing light from a 450-W Xe-arc lamp (Ushio, UXL-451-0) was collected by a focusing lens and directed through a grating monochromator (Nikon, G250) to a silicon avalanche photodiode detector (Hamamatsu Photonics, S5343). The transient signals were recorded with a digitizer (Tektronix, TDS 580D). The reported signals are averages of 2−4 events. The excitations of the $PySA^-$-loaded Nafion membranes in the solutions were carried out in 1-mm quartz cells. The analyzing lamp, sample, monochromator, and a silicon avalanche photodiode detector all lie on the same axis with the excitation beam incident at 45° to the axis. All measurements were carried out at room temperature.

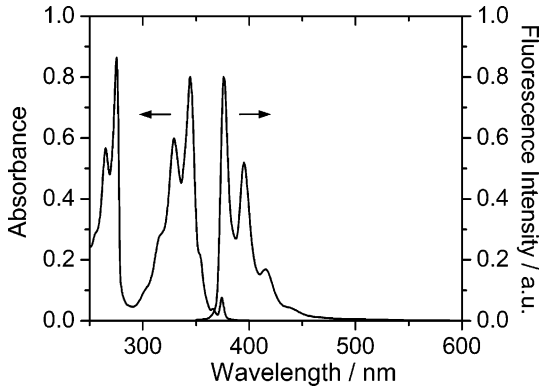

Figure 1. UV/visible absorption and fluorescence spectra observed for the $PySA^-$-loaded Nafion-H^+ membrane. No excimer band for $PySA^-$ was observed.

Results and Discussion

Resonant Two-Photon Ionization of $PySA^-$ in Nafion. The UV/visible absorption and fluorescence spectra of $PySA^-$ in the dry Nafion membrane are shown in Figure 1. The average $PySA^-$ concentration within the membrane was estimated to be about 1.3×10^{-3} M by using the molar absorbance coefficient (ϵ) of $PySA^-$ in water ($\epsilon = 34\,000$ M^{-1} cm^{-1} at 346 nm) and its thickness (0.18 mm). In a way similar to that of Py, the I_3/I_1 value has been shown to increase with decreasing solvent polarity, ranging in values from 0.51 in water to 0.82 in perfluoro-1,4-dimethylcyclohexane.[12] In the present systems, an I_3/I_1 value of 0.65 $\pm$ 0.1 was determined, suggesting that $PySA^-$ is located on the fluorocarbon side of the fluorocarbon−ionic cluster interfacial region as mentioned elsewhere.[14] It should also be noted that no excimer band for $PySA^-$ was observed.

Figure 2A shows the transient absorption spectra observed after the laser flash during the 355-nm laser photolysis (10 mJ pulse^{-1}) of the $PySA^-$-loaded Nafion-H^+ membrane immersed in water (pH 7). The absorption band with a peak at about 460 nm is attributable to $Py^{\bullet+}SA^-$.[16] As shown in Figure 2B, the log−log plot of ΔOD at 460 nm observed at 500 ns after the laser flash and laser fluence (F) showed a linear relationship with a slope of 1.2 $\pm$ 0.1, suggesting that the resonant two-photon ionization of $PySA^-$ generates $Py^{\bullet+}SA^-$ via the CT excited state analogous to that in the bulk water.[16] With use of the ϵ value of $Py^{\bullet+}SA^-$ ($(3.5 \pm 0.3) \times 10^4$ M^{-1} cm^{-1} at 460 nm in water),[20] the concentration of the generated $Py^{\bullet+}SA^-$ ($[Py^{\bullet+}SA^-]$) was calculated to be $(2.5 \pm 0.4) \times 10^{-4}$ M. We also examined the generation of $Py^{\bullet+}SA^-$ during the 355-nm laser photolysis (10 mJ pulse^{-1}) of air-saturated water containing $PySA^-$ (1×10^{-4} M) and determined the $[Py^{\bullet+}SA^-]$ to be $(1.4 \pm 0.2) \times 10^{-5}$ M. The lifetimes of $Py^{\bullet+}SA^-$, which are evaluated as the time required for 50% of the initial ΔOD values, were estimated to be 23 and 1.3 μs for the Nafion-H^+ membrane and the bulk water, respectively. The lifetimes of $Py^{\bullet+}SA^-$ should be dependent on the charge recombination rates between $Py^{\bullet+}SA^-$ and hydrated electrons (e_{aq}^-), the dimerization reaction rate to yield the dimer radical cation ($(PySA^-)_2^{\bullet+}$), and the quenching rate by oxygen in water. However, no absorption bans attributed to $(PySA^-)_2^{\bullet+}$ and e_{aq}^- were observed in the wavelength range (600−1800 nm) and time resolution (5 ns). The concentrations of oxygen, $PySA^-$, and $Py^{\bullet+}SA^-$ in the Nafion-H^+ membrane are relatively high, compared with those in the bulk water. In particular, the solubility of oxygen in the Nafion membrane (10.7×10^{-3} M) is much higher than that in water (1.3×10^{-3} M).[21] Almost the same time traces were also

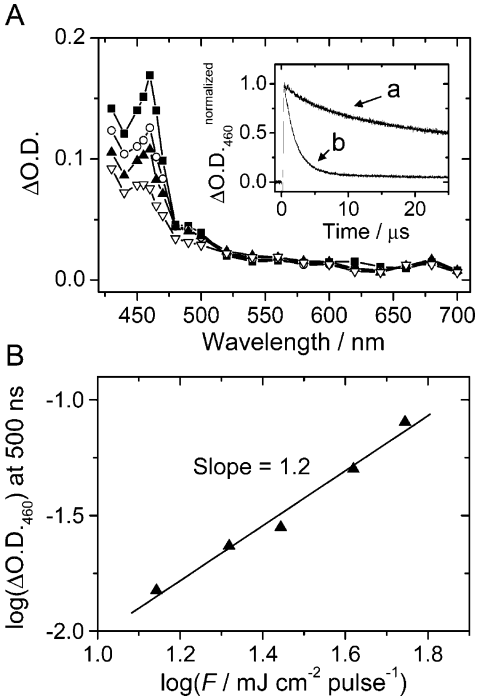

Figure 2. Transient absorption spectra observed at 0.5 (solid squares), 5 (open circles), 10 (solid triangles), and 20 (open inverted triangles) μs after the laser flash during the 355-nm laser photolysis of the $PySA^-$-loaded Nafion-H^+ membrane immersed in air-saturated water (A). Inset: Time traces at 460 nm observed during the 355-nm laser photolysis of the $PySA^-$-loaded Nafion-H^+ membrane immersed in air-saturated water (a) and $PySA^-$ (1×10^{-4} M) in air-saturated water (pH 7) (b). Log−log plots of ΔOD at 460 nm vs laser fluence (F in mJ cm^{-2} per pulse).

observed during the laser photolysis of the $Py^{\bullet+}SA^-$-loaded Nafion-Na^+ membrane, indicating that Na^+ does not quench the $Py^{\bullet+}SA^-$ in the present time domain. In addition, no absorption band due to e_{aq}^- was observed during the laser photolysis of the $Py^{\bullet+}SA^-$-loaded Nafion-Na^+ membrane. Therefore, the observed long lifetime of $Py^{\bullet+}SA^-$ in the Nafion-H^+ membrane is mainly attributed to the suppression of the charge recombination process because of the fast scavenging of e_{aq}^- by the fluorocarbon part of the Nafion-H^+ membrane. The observed absorption band monotonically increased with a shorter wavelength in the wavelength region of 430−500 nm, indicating the generation of long-lived species such as alkyl chain radicals (see the spectrum observed at 20 μs shown in Figure 2A).[22]

Quenching Process of $Py^{\bullet+}SA^-$ by Nucleophilic Anions in Nafion. To clarify the reactivities of anions in the Nafion membrane, we examined the decay kinetics of $Py^{\bullet+}SA^-$ in the presence of nucleophilic anions in the Nafion-H^+ membrane and the bulk water.

Figure 3 shows the transient absorption spectra and the time traces at 460 nm observed during the laser photolysis of the $Py^{\bullet+}SA^-$-loaded Nafion-H^+ membrane immersed in water in the absence and presence of NaI. The lifetimes of $Py^{\bullet+}SA^-$ significantly decreased with the increasing NaI concentration as shown in Figure 3B. The experimental results clearly indicate that $Py^{\bullet+}SA^-$ was quenched with the addition of NaI in the Nafion-H^+ membrane.

This quenching process of $Py^{\bullet+}SA^-$ is due to the electron transfer from nucleophilic anions (X^-) to $Py^{\bullet+}SA^-$ as given by eq 1.[23]

$$Py^{\bullet+}SA^- + X^- \rightarrow PySA^- + X^{\bullet} \qquad (1)$$

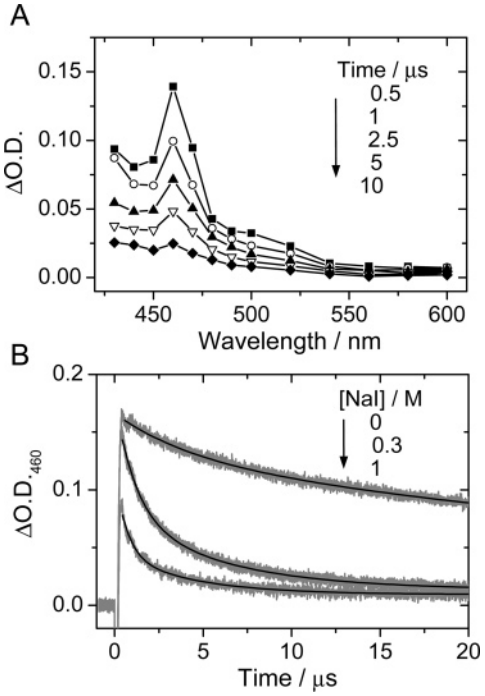

Figure 3. Transient absorption spectra observed at 0.5 (solid squares), 2 (solid triangles), 10 (open inverted triangles), and 20 (solid diamonds) μs after the laser flash during the 355-nm laser photolysis of the $PySA^-$-loaded Nafion-H^+ membrane immersed in water in the presence of NaI (0.3 M) (A). Time traces at 460 nm observed during the 355-nm laser photolysis of the $PySA^-$-loaded Nafion-H^+ membrane immersed in water in the absence and presence of NaI.

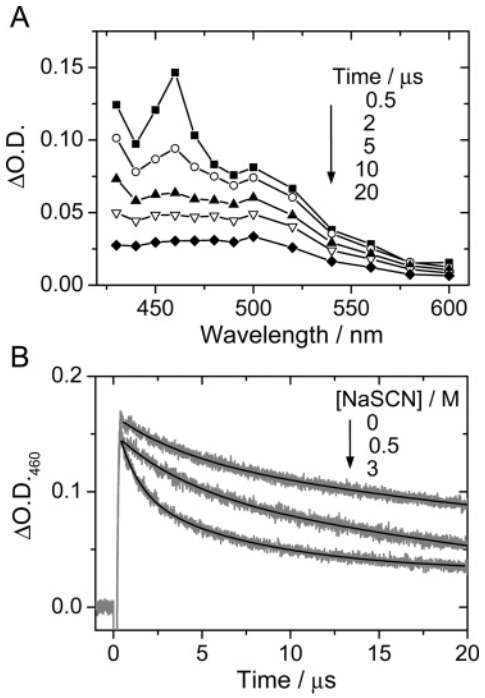

Figure 4. Transient absorption spectra observed at 0.5 (solid squares), 2 (open circles), 10 (open inverted triangles), and 20 (solid diamonds) μs after the laser flash during the 355-nm laser photolysis of the $PySA^-$-loaded Nafion-H^+ membrane immersed in water in the presence of NaSCN (3 M) (A). Time traces at 460 nm observed during the 355-nm laser photolysis of the $PySA^-$-loaded Nafion-H^+ membrane immersed in water in the absence and presence of NaSCN.

Figure 4 shows the transient absorption spectra and the time traces at 460 nm observed during the laser photolysis of the

TABLE 1: The Quenching Rate Constants of $Py^{\bullet+}SA^-$ by Several Ions in the Nafion-H^+ Membrane (k_q^{Nf}) and the Bulk Water (k_q^{Nf}) and Physical Properties of Anions

quencher	ΔG_{ET},[a] eV	k_q^{Nf},[b] 10^6 M^{-1} s^{-1}	k_q^{bulk}, 10^9 M^{-1} s^{-1}	AF[c]	r,[d] nm	$\Delta G°_{hyd}$,[e] kJ mol^{-1}	$\Delta G°_{tr}$,[f] kJ mol^{-1}	D,[g] 10^{-9} m^2 s^{-1}
N_3^-	−0.13	3.7	7.2[b]	−3.3	0.195	−287	NA[h]	1.837
Br^-	−0.18	0.032	0.26[a]	−3.9	0.196	−321	+38	2.08
SCN^-	−0.68	0.18	0.04[b]	−2.5	0.213	−287	+19	1.758
I^-	−0.81	0.16	7.9[a]	−3.6	0.220	−283	+25	2.045

[a] Reference 23. [b] This work. [c] Defined as $\log(k_q^{Nf}/k_q^{bulk})$. [d] Ionic radius, ref 27. [e] Standard molar Gibbs free energy change of hydration at 298.15 K, ref 27. [f] Standard molar Gibbs free energy change of transfer from water to 1,2-dichloroethane at 298.15 K. [g] Self-diffusion coefficient in water at 298.15 K, ref 27. [h] Not available.

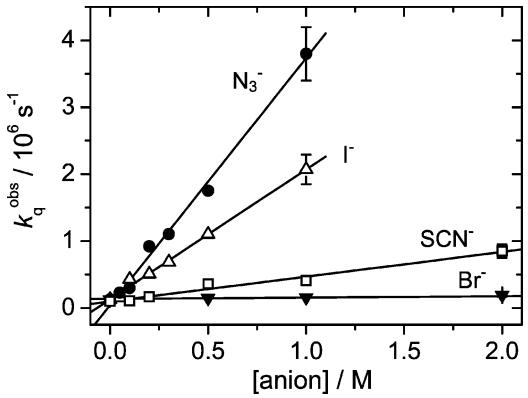

Figure 5. Anion concentration dependences of the observed quenching rate constants (k_q^{obs}) during the 355-nm laser flash photolysis of the $PySA^-$-loaded Nafion membrane immersed in water in the absence and presence of salts.

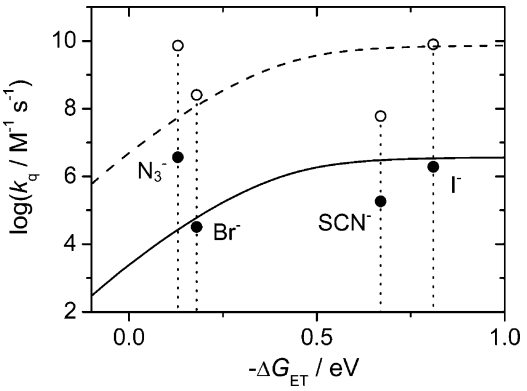

Figure 6. The relationship between the driving force (ΔG_{ET}) for the electron transfer from anions to $Py^{\bullet+}SA^-$ and k_q obtained in the Nafion-H^+ membrane (solid circles) and the bulk solution (open circles). Broken lines indicate the calculated k_q values from eqs 5−8. The solid line is a guide for the eyes.

$Py^{\bullet+}SA^-$-loaded Nafion-H^+ membrane immersed in water in the absence and presence of NaSCN. The lifetimes of $Py^{\bullet+}SA^-$ significantly decreased with the increasing NaSCN concentration as shown in Figure 4B. As shown in Figure 4A, an absorption band with a broad peak around 460−500 nm was observed at 20 μs after the laser flash. This absorption band is attributable to $(SCN)_2^{\bullet-}$, which is generated by the dimerization reaction between $SCN^\bullet$ and SCN^- as given by eqs 2 and 3

$$Py^{\bullet+}SA^- + SCN^- \rightarrow PySA^- + SCN^\bullet \quad (2)$$

$$SCN^\bullet + SCN^- \rightleftarrows (SCN)_2^{\bullet-} \ (K_{eq} = 2.5 \times 10^5\ M^{-1}) \quad (3)$$

where K_{eq} is the formation constant of $(SCN)_2^{\bullet-}$.[24] By using the ϵ value of 7580 M^{-1} cm^{-1} at 472 nm for $(SCN)_2^{\bullet-}$,[25,26] the yield of $(SCN)_2^{\bullet-}$, which is represented by $[(SCN)_2^{\bullet-}]/[Py^{\bullet+}SA^-]$, is calculated to be about 0.8 at [NaSCN] = 3 M, suggesting that a large part of $Py^{\bullet+}SA^-$ in the Nafion-H^+ membrane was quenched by SCN^- via the electron-transfer process (eq 2).

Assuming a quasi-first-order reaction for a quenching process, the observed quenching rate ($k_q^{obs} = k_q[Q]$) was simulated by eq 4,

$$\frac{d[Py^{\bullet+}SA^-]}{dt} = -k_q[Py^{\bullet+}SA^-][Q] - k_0[Py^{\bullet+}SA^-] \quad (4)$$

where Q is the quencher and k_0 is the deactivation rate of $Py^{\bullet+}SA^-$. The plots of k_q^{obs} vs anion concentration ([anion]) are represented in Figure 5. The linear relationship between the k_q^{obs} values and [anion] indicates that no complex between $Py^{\bullet+}SA^-$ and anions was formed in the present substrate concentration.

The apparent k_q values obtained in the Nafion-H^+ membrane (k_q^{Nf}), which are determined from the linear relationship between the k_q^{obs} values and [anion], are listed in Table 1 with those obtained in the bulk water (k_q^{bulk}) and the physical properties of the anions.

Electron-Transfer Reaction Mechanism. Figure 6 shows the $-\Delta G_{ET}$ dependences of log k_q^{Nf} (solid circles) and log k_q^{bulk} (open circles).

With use of steady-state approximation and assumptions, the overall k_q is given by eq 5,[28]

$$\frac{1}{k_q} = \frac{1}{k_D} + \frac{1}{k_{ET}} \quad (5)$$

where k_D and k_{ET} are the diffusion-controlled and the electron-transfer reaction rate constants, respectively. The k_{ET} can be calculated by using the Jortner and Bixon formalism ,which treats the vibrational high-frequency modes quantum mechanically as given by eq 6,[29]

$$k_{Et} = \sqrt{\frac{\pi}{\hbar^2 \lambda_s k_B T}}\, V(r)^2 \sum_{j_A, j_D} FC(j_A) FC(j_D) \times \exp\left\{ -\frac{(\lambda_s + \Delta G_{ET} + j_D h\nu_D + j_A h\nu_A)^2}{4\lambda_s k_B T} \right\} \quad (6)$$

where $\hbar$ is Planck's constant divided by 2π, k_B is Boltzmann's constant, T is the absolute temperature, λ_s is the solvent reorganization energy, $j_D h\nu_D$ and $j_A h\nu_A$ are the intramolecular reorganization energy for the electron donor and acceptor, respectively, ΔG_{ET} is the free energy change of the electron-transfer reaction, and $V(r)$ is the electronic coupling element

between electron donor and acceptor dependent on the distance between these species as given by eq 7,

$$V(r) = V_0 \exp\left\{-\frac{\beta}{2}(r - r_0)\right\} \quad (7)$$

where V_0 is the V at the contact distance (r_0) and β is the decay parameter. Solvent reorganization energy (λ_s) for the electron transfer is given by eq 8,

$$\lambda_s = \frac{e^2}{4\pi\epsilon_0}\left(\frac{1}{2r_D} + \frac{1}{2r_A} - \frac{1}{d_{DA}}\right)\left(\frac{1}{{n_D}^2} - \frac{1}{\epsilon}\right) \quad (8)$$

where r_D and r_A are the radii of the electron donor and acceptor, respectively, and d_{DA} is the distance between the electron donor and acceptor ($d_{DA} = r_D + r_A$). The permittivity constant of a vacuum, the refractive index, and the dielectric constant of the solvent are represented by ϵ_0, n_D, and ϵ, respectively ($n = 1.333$ and $\epsilon = 80.16$ for water). By using a molecular radius r_D of 0.20 nm and r_A of 0.42 nm for anions and $Py^{\bullet+}SA^-$, respectively,[27,30] λ_s was calculated to be 0.82 eV from eq 8. This λ_s value is quite consistent with that reported elsewhere.[23]

To calculate the k_{ET} values, we used a value of $j_D h\nu_D$ ($j_A h\nu_A$) = 0.25 eV,[23] which is similar to the value of 0.29 eV reported by Myers and co-workers, and the average frequency ν_D (ν_A) of 1400 cm^{-1} to represent the high-frequency intramolecular modes.[31] Using $V_0 = 40$ cm^{-1},[23] $\beta = 11$ nm^{-1},[32] and $k_D = 7.6 \times 10^9$ M^{-1} s^{-1}, we obtained the calculated k_q values from eqs 5−8 as shown by the broken line in Figure 6.

It is noted that the observed k_q^{Nf} values were considerably lower than the k_q^{bulk} values by a factor of 10^2-10^4 (see the solid line in Figure 6). If the effects of the steric hindrance and the polarity of the fluorocarbon part of the Nafion-H^+ membrane on the parameters such as $V(r)$, k_D, and λ_s are ruled out, the significant decreases in k_q are mainly due to the local concentration and/or mobility of the anions in the Nafion membrane. As mentioned in the Introduction, anionic species cannot easily diffuse into the Nafion membrane due to the negatively charged $-SO_3^-$ group, while cationic species can easily diffuse into the Nafion membrane. In fact, when Fe^{2+} was used as a quencher, a relatively large k_q^{Nf} value (8.0×10^8 M^{-1} s^{-1}) was observed, compared with k_q^{bulk} (2.7×10^8 M^{-1} s^{-1}).

Hofmeister Effects on the Electron-Transfer Reactions. As shown in Figure 6, the k_q^{Nf} values were substantially lower than the k_q^{bulk} values by a factor of 10^2-10^4. In addition, it seems that the decrease in k_q significantly depends on the nature of the anions. Here, to discuss such differences between anions, we use the attenuation factor (AF) as $\log(k_q^{Nf}/k_q^{bulk})$. The determined AFs decreased in the order $SCN^- > N_3^- > I^- > Br^-$ as summarized in Table 1. The electron-transfer perturbation by Nafion environment cannot explain all observed data, and the Hofmeister effect should be considered.

As is well-known, the Hofmeister series plays a significant role in a dramatic range of biological and physicochemical phenomena, affecting the solubility of hydrophobic solutes in water, the cloud points of the polymer and surfactant solutions, the action of ions on ion channels, the activities of various enzymes, and the surface tension of electrolyte solutions.[33−35] Typical Hofmeister series are as follows: $ClO_4^- > SCN^- > I^- > NO_3^- > Br^- > Cl^- > CH_3COO^- > HCOO^- > F^- > OH^- > HPO_4^{2-} > SO_4^{2-}$.

For example, SCN^- is relatively large in size and hydrophobic in nature, compared to Br^-. Therefore, Br^- may well be located in the aqueous core region of the Nafion membrane as shown in Figure 7. The more hydrophobic ions such as SCN^- might be expected to be located in the more hydrophobic interfacial region. On the other hand, it is likely that $PySA^-$ is located on the fluorocarbon side of the fluorocarbon-ionic cluster interfacial region because of the highly hydrophobic nature of the Py chromophore. This leads to the suggestion that hydrophobic ions such as SCN^- are more likely to be found in the vicinity of $Py^{\bullet+}SA^-$ in the fluorocarbon−water interfacial region. The fact that the AF obtained for Br^- is considerably small compared with that obtained for SCN^- is probably due to the average distance between $Py^{\bullet+}SA^-$ and anions. Unfortunately, we cannot compare the AF for SCN^-, N_3^-, I^-, and Br^- with that for Cl^-, which is the most hydrophilic halogen ion, because no quenching of $Py^{\bullet+}SA^-$ was observed in the presence of NaCl (1 M).

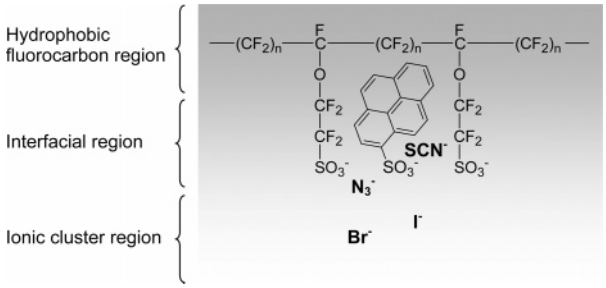

Figure 7. Schematic representation of the location of different ions within the wet $PySA^-$-loaded Nafion membrane.

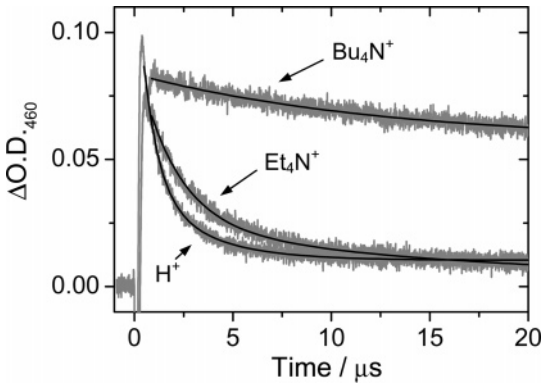

Figure 8. Time traces at 460 nm observed during the 355-nm laser photolysis of the $PySA^-$-loaded Nafion-H^+, Et_4N^+, and Bu_4N^+ membranes immersed in water in the presence of NaN_3 (0.2 M).

Effects of Hydrophobic Organic Cations. When large hydrophobic organic cations such as Bu_4N^+ and Et_4N^+ were exchanged into the Nafion membranes, the membrane structure was totally controlled by these organic cations, and consequently, it is expected to control the local [anion].

Figure 8 shows the effects of Et_4N^+ and Bu_4N^+ exchanged into the Nafion membranes on the quenching kinetics of $Py^{\bullet+}SA^-$ in the presence of NaN_3 (0.2 M). The k_q^{obs} values of $Py^{\bullet+}SA^-$ significantly decreased in the order $H^+ > Et_4N^+ > Bu_4N^+$ as summarized in Table 2.

As summarized in Table 2, $PySA^-$ concentrations in the Nafion membranes were estimated to be 1.3×10^{-3}, 1.0×10^{-3}, and 0.7×10^{-3} M for the Nafion-H^+, -Et_4N^+, and -Bu_4N^+ membranes, respectively. The decrease in [$PySA^-$] with the increasing size of the cations suggests that large bulky hydrophobic organic cations inhibit the incorporation of $PySA^-$ molecules into the fluorocarbon side of the fluorocarbon−ionic cluster interfacial region. In addition, as shown in Figure 8, the quenching kinetics of $Py^{\bullet+}SA^-$ significantly depend on the size

TABLE 2: The [$PySA^-$] in Nafion Membranes and k_q^{obs} Values Obtained for $Py^{\bullet+}SA^-$-Loaded Nafion-H^+, -Et_4N^+, and -Bu_4N^+ Membranes in the Presence of NaN_3 (0.2 M) and Physical Properties of Cations

cation	[$PySA^-$], M	k_q^{obs}, s^{-1} ($\log k_q^{obs}$, s^{-1})	r,[a] nm	V^∞,[b] $cm^3\ mol^{-1}$
H^+	1.3×10^{-3}	1.1×10^6 (6.0)	0.030	−5.5
Et_4N^+	1.0×10^{-3}	4.4×10^5 (5.6)	0.337	143.6
Bu_4N^+	0.7×10^{-3}	6.6×10^4 (4.8)	0.417	270.2

[a] Ionic radius, ref 27. [b] Standard partial molar volume of the ion in water at 298.15 K, ref 27.

of the organic cations. Similar inhibiting effects were observed for other anions in the Nafion-Bu_4N^+ membrane and for the salts having Bu_4N^+ as a countercation in the Nafion-H^+ membrane. These results clearly suggest that one can control the incorporation of anions into the Nafion membrane using large hydrophobic organic cations. The electron transfer from anions to $Py^{\bullet+}SA^-$ occurs at the fluorocarbon−ionic cluster interfacial region, but not in the ionic cluster region of the Nafion membrane.

Conclusions

The electron-transfer reaction from nucleophilic anions such as SCN^-, N_3^-, I^-, and Br^- to $Py^{\bullet+}SA^-$ generated via a resonant two-photon ionization process in the Nafion membranes was investigated with transient absorption measurements. The apparent quenching rates observed in Nafion (k_q^{Nf}) were almost 2−4 orders smaller than those observed in the bulk solutions (k_q^{bulk}). The attenuation factor (AF), which is defined as $\log(k_q^{Nf}/k_q^{bulk})$, decreased in the order $SCN^- > N_3^- > I^- > Br^-$. According to the anionic Hofmeister effects, the hydrophobic ions such as SCN^- are more likely to be found in the vicinity of $Py^{\bullet+}SA^-$ in the fluorocarbon−ionic cluster interfacial region. Hydrophobic organic cations such as Bu_4N^+ and Et_4N^+ exchanged into the Nafion membranes inhibit the incorporation of anions into the Nafion membrane.

Acknowledgment. This work has been partly supported by a Grant-in-Aid for Scientific Research on Priority Area (417), 21st Century COE Research, and others from the Ministry of Education, Culture, Sports, Science and Technology (MEXT) of the Japanese Government.

References and Notes

(1) Heitner-Wirguin, C. *J. Membr. Sci.* **1996**, *120*, 1.
(2) Lehmani, A.; Turq, P.; Perie, M.; Perie, J.; Simonin, J.-P. *J. Electroanal. Chem.* **1997**, *428*, 81.
(3) Samec, Z.; Trojanek, A.; Langmaier, J.; Samcova, E. *J. Electrochem. Soc.* **1997**, *144*, 4236.
(4) Okada, T.; Xie, G.; Gorseth, O.; Kjelstrup, S.; Nakamura, N.; Arimura, T. *Electrochim. Acta* **1998**, *43*, 3741.
(5) (a) Verbrugge, M. W.; Hill, R. F. *J. Electrochem. Soc.* **1990**, *137*, 886. (b) Verbrugge, M. W.; Hill, R. F. *J. Electrochem. Soc.* **1990**, *137*, 893.
(6) Capeci, S. W.; Pintauro, P. N.; Bennion, D. N. *J. Electrochem. Soc.* **1989**, *136*, 2876.
(7) Pourcelly, G.; Lindheimer, A.; Gavach, C. *J. Electroanal. Chem.* **1991**, *305*, 97.
(8) Sodaye, H. S.; Pujari, P. K.; Goswami, A.; Manohar, S. B. *J. Radioanal. Nucl. Chem.* **1996**, *214*, 399.
(9) Hurst, J. K.; Khairutdinov, R. F. In *Electron Transfer in Chemistry*; Wiley-VCH: New York, 2001; Vol. 4, p 578.
(10) Kuczynski, J. P.; Milosavljevic, B. H.; Thomas, J. K. *J. Phys. Chem.* **1984**, *88*, 980.
(11) Lee, P. C.; Meisel, D. *Photochem. Photobiol.* **1985**, *41*, 21.
(12) Szentirmay, M. N.; Prieto, N. E.; Martin, C. R. *J. Phys. Chem.* **1985**, *89*, 3017.
(13) Blatt, E.; Launikonis, A.; Mau, A. W.-H.; Sasse, W. H. F. *Aust. J. Chem.* **1987**, *40*, 1.
(14) Robertson, M. A. F.; Yeager, H. L. *Macromolecules* **1996**, *29*, 5166.
(15) Hu, Q. D. Y.; Moore, R. B.; McCormick, C. L.; Mauritz, K. A. *Chem. Mater.* **1997**, *9*, 36.
(16) Hara, M.; Tojo, S.; Kawai, K.; Majima, T. *Phys. Chem. Chem. Phys.* **2004**, *6*, 3215.
(17) Kiwi, J.; Dhananjeyan, M. R.; Nadtochenko, V. *J. Phys. Chem. A* **2002**, *106*, 7138.
(18) Liu, P.; Bandara, J.; Lin, Y.; Elgin, D.; Allard, L. F.; Sun, Y.-P. *Langmuir* **2002**, *18*, 10398.
(19) John, S. A.; Ramaraj, R. *J Appl. Polym. Sci.* **1997**, *65*, 777.
(20) (a) We determined the ϵ value of $Py^{\bullet+}SA^-$ at 460 nm in water using the ϵ value of e_{aq}^- at 720 nm ($1.85 \times 10^4\ M^{-1}\ cm^{-1}$).[20b] (b) *CRC Handbook of Radiation Chemistry*; Tabata, Y., Ito, Y., Tagawa, S., Eds.; CRC Press: Boca Raton, FL, 1991.
(21) Ogumi, Z.; Kuroe, T.; Takehara, Z. *J. Electrochem. Soc.* **1985**, *132*, 2601.
(22) Szadkowska-Nicze, M.; Mayer, J. *Radiat. Phys. Chem.* **1999**, *56*, 553.
(23) Koike, K.; Thomas, J. K. *J. Chem. Soc., Faraday Trans.* **1992**, *88*, 195.
(24) Hurley, J. K.; Linschitz, H.; Treininl, A. *J. Phys. Chem.* **1988**, *92*, 5151.
(25) Schuler, R. H.; Patterson, L. K.; Janata, E. *J. Phys. Chem.* **1980**, *84*, 2088.
(26) Hug, G. L. *Optical Spectra of Non-Metallic Inorganic Transient Species in Aqueous Solution*; NSRDS-NBS 69; 1981.
(27) Marcus, Y. *Ion properties*; Marcel Dekker: New York, 1997.
(28) Kavarnos, G. J.; Turro, N. J. *Chem. Rev.* **1986**, *86*, 401.
(29) (a) Marcus, R. A.; Sutin, N. *Biochim. Biophys. Acta* **1985**, *811*, 265. (b) Bixon, M.; Jortner, J.; Cortes, J.; Heitele, H.; Michel-Beyerle, M. E. *J. Phys. Chem.* **1994**, *98*, 7289.
(30) The molecular radius (r) for $PySA^-$ was obtained from the density functional theory (DFT) with the GAUSSIAN 98 suite of programs. Molecular volume of the solute was calculated by the B3LYP density functional with the standard 6-31G* basis set (B3LYP/6-31G* Volume). The r value was determined under the assumption that the solute molecule is a sphere.
(31) Markel, F.; Ferris, N. S.; Gould, I. R.; Myers, A. B. *J. Am. Chem. Soc.* **1992**, *114*, 6208.
(32) Tavernier, H. L.; Kalashnikov, M. M.; Fayer, M. D. *J. Chem. Phys.* **2000**, *113*, 10191.
(33) Hofmeister, F. A*rch. Exp. Pathol. Pharmakol.* **1888**, *24*, 247.
(34) Collins, K. D.; Washabaugh, M. W. *Q. Rev. Biophys.* **1985**, *18*, 323.
(35) Cacace, M. G.; Landau, E. M.; Ramsden, J. J. *Q. Rev. Biophys.* **1997**, *30*, 241.